

- from *eryAI* is present between the Xcm I and Eco RI sites upstream of *Tc*. The sequence between the Xcm I and Bsi WI sites is 5'-CCATCGTGGG-GATCCTCTAGGTACG-3'.
29. T. Maniatis, E. F. Fritsch, J. Sambrook, *Molecular Cloning: A Laboratory Manual* (Cold Spring Harbor Laboratory, Cold Spring Harbor, NY, 1982).
30. D. J. MacNeil, *J. Bacteriol.* 170, 5607 (1988).

31. In these experiments, propionic acid was neutralized with sodium hydroxide.
32. L. Katz, unpublished results.
33. J. G. Nourse and J. D. Roberts, *J. Am. Chem. Soc.* 97, 4584 (1975).
34. We thank S. R. Kushner for providing us with pMAK705 and J. I. Brauman and D. A. Hopwood for helpful comments on the manuscript. Support-

ed in part by grants from NSF (BCS-9209901) and the American Cancer Society (IRG-32-34) to C.K. and by a Camille and Henry Dreyfus New Investigator Award to C.K. C.M.K. is a recipient of a Department of Defense National Defense Science and Engineering Graduate Fellowship.

1 April 1994; accepted 31 May 1994

Creation of Liquid Crystal Waveguides with Scanning Force Microscopy

M. Rüetschi, P. Grütter,* J. Fünfschilling,† H.-J. Güntherodt

The rubbing of a polymer layer, a commonly applied process, leads to an anisotropic surface morphology, aligning liquid crystal molecules. Scanning force microscopy can be used to intentionally create areas with a similar anisotropy by operating the instrument at loads in the range of 10^{-7} to 10^{-5} newtons. These areas have an orientation effect on liquid crystals indistinguishable from the rubbing process, which allows a systematic investigation of the orientation properties of an alignment layer as a function of its nanometer-scale morphology. Refractive index patterns can be tailored with this method by scratching a suitable area, as demonstrated by fabrication of an optical waveguide 6 micrometers wide and 5 millimeters long.

Light-guiding structures play an important role in modern optics-based communication systems. Today, most of these devices are fabricated from glassy materials or from single crystals. Few attempts have been made to use liquid crystals (LCs), mainly because their switching speeds (microsecond to millisecond) are many orders of magnitude too slow to compete with conventional electrooptic materials. Recently, however, LCs with large optical nonlinearity have been found (1) that are extremely fast, so fast that they even act as diodes for light frequencies, leading to frequency-doubled light (second harmonic generation). The construction of an ultrafast nonlinear optical LC switching device (for example, a Mach-Zehnder interferometer) would require the development of methods for the production of light-guiding structures in LC layers. As an approach to this problem, we used a scanning force microscope (SFM) (2) as a tool to produce orientation patterns for light guiding in LCs.

The basic structure of a light-guiding LC layer is very similar to the familiar LC display (LCD): two glass plates separated by several micrometers with the LCs sandwiched in between. The glass plates have transparent electrodes and are, in addition, covered by thin polymer layers, which align the LC material. This alignment property is achieved by unidirectionally rubbing the

polymer layer with a velvet roller. This technique is widely used in LCD fabrication and leads to a uniform orientation of the LC molecules near that surface. The mechanism responsible for the orientation is still uncertain (3).

A lot of work has been done on the modification of polymer surfaces with an SFM. The fabrication of grooves on various polymer surfaces with an SFM has been reported by a number of authors (4). These grooves look very similar to the grooves created by rubbing (5). We used an SFM to modify the polymer surface in a highly controlled manner to investigate how these modifications affect LC orientation. We found that by varying parameters such as loading, scan speed, and line density, different degrees of orientation can be achieved. This allows us to systematically investigate the LC orientation properties of a substrate as a function of morphology. The refractive index of the LC layer can also be manipulated on the micrometer scale by selecting a suitable SFM scratching pattern.

The SFM measurements were carried out with a commercially available instrument (6) operated in the constant-force mode under ambient conditions at room temperature. Microfabricated force sensors with spring constants of 0.12 and 3 N/m were used. The SFM was operated in two different modes: an imaging mode (loading force of about 10^{-9} N) and a surface modification mode (loading force, 10^{-7} to 10^{-5} N), which we will term scratching. Scratching on a larger scale was performed with a home-built instrument capable of scanning a force sensor over a 80 μm by 10 mm area. Movements in the small

direction are achieved with a piezoelectric bimorph. This scanner is attached to a commercial motorized translation stage, enabling movements in the large direction at uniform scan speeds from 3.6 to 50 $\mu\text{m/s}$.

As samples, we used glass plates covered with a 25-nm thin layer of sputtered InSnO (ITO) onto which a 5- to 25-nm thin nylon layer was spin-coated. After deposition, the nylon layer was rubbed with a velvet roller and additionally scratched. Subsequently, an LC cell was made by mounting this plate together with a regularly rubbed nylon-coated glass plate. The rubbing directions on both plates were selected to be parallel. The spacing of the glass plates was fixed at about 6 μm by glass fiber cuts of the same diameter. The cell was filled with a nematic LC mixture with a refractive index parallel and perpendicular to the nematic director of 1.65 and 1.5, respectively. Additionally, optical properties of LC cells were investigated by polarizing microscopy to study the LC orientation.

Figure 1 shows an SFM image of a rubbed nylon orientation layer; the area in the top left part of the figure was additionally scratched by the SFM. The bright areas can be identified as nylon. The striations (or grooves) visible parallel to the rubbing direction R are caused by the rubbing pro-

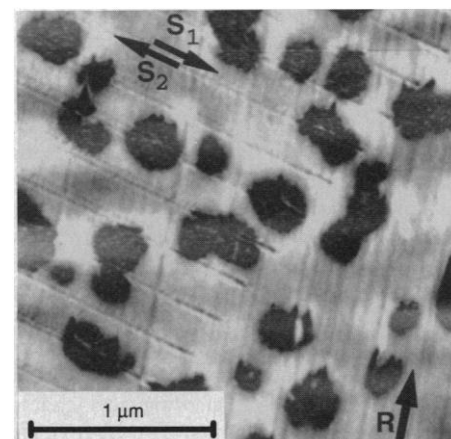


Fig. 1. An SFM image of a rubbed nylon layer that was also scratched. The picture was acquired at a tip loading of about 10^{-9} N. The rubbing direction is marked by arrow R. The area in the top left corner shows scratches made by the SFM at a load of 10^{-7} N. The scratches made in forward and backward direction are marked as arrows S_1 and S_2 , respectively.

Institute of Physics, University of Basel, Klingelbergstrasse 82, CH-4056 Basel, Switzerland.

*Present address: Physics Department, McGill University, 3600 rue University, Montreal, H3A 2T8, Canada.
†Present address: F. Hoffmann-La Roche, Ltd., RLCR 64/116, CH-4002 Basel, Switzerland.

cess. Typically, the grooves have a separation of 50 nm, an average width of 20 nm, and a depth of about 1 to 2 nm. The dark hole-like regions showing no striation are regions of ITO not covered by nylon. The scratches visible in the top left part of the figure were made by the SFM at a tip loading of 10^{-7} N. The scratches are 26 nm wide, 2 to 5 nm deep, and 240 nm apart.

The manipulation of surface morphology by the SFM opens an experimental field for the investigation of orientation mechanisms of LCs. One can macroscopically observe and quantify the alignment effects of scanning at high loads by fabricating an LC cell after scratching the upper plate at an angle θ with

respect to the nylon rubbing direction. Surprisingly, the regions scratched by the SFM can be seen as rectangles with a brightness that differs from the background when the cell is viewed in a polarizing microscope, even if the scratches made by the SFM are only a few nanometers wide and 135 nm apart.

The LC molecules are parallel to the rubbing direction in areas where the upper surface is not scratched (Fig. 2A). As a result, the polarization of light passing through these regions is not rotated. This leads to a dark display under crossed polarizers. When the upper surface is scratched at an angle θ to the rubbing direction (Fig. 2B), the LC molecules near the upper layer are forced into a new direction. This direction is normally not the same as the scratching direction. The areas between the scratches are still dominated by the rubbing direction if the distance between two individual scratches is not too small (Fig. 1). As a consequence, LC molecules align along a direction given by the angle ϕ , which is normally smaller than θ . However, this leads to a twisted nematic (TN) structure of the LC. The polarization of light polarized parallel to the LC orientation at the entrance of the glass surface is rotated by the angle ϕ when transmitted through the cell. This leads to a bright area on a dark background. The effectively observed contrast depends on the relative orientation of polarizer and analyzer. Thus, it is also possible to achieve a dark scratched region on a bright background.

The angle ϕ is related to the orientation efficiency of the scratched nylon morphology. It increases with increasing orientation efficiency of the scratches and reaches a

maximum (strong anchoring) at $\phi = \theta$. To study the orientation efficiency of the scratches, we measured the rotation angle ϕ with a polarizing microscope as a function of the applied force F , the line separation d , and the scan velocity v . Because the morphology of the nylon surface varies somewhat from sample to sample, we studied the ϕ dependence of a particular parameter on the same sample.

We found ϕ , and thus the orientation efficiency, to increase with higher F , smaller d , and smaller v (Fig. 3). With sufficiently high F ($>10^{-6}$ N), ϕ is independent of the scan velocity. At this large force, we achieve $\phi = \theta$ (that is, maximum orientation efficiency) if $d \leq 50$ nm. Generally, we find maximal orientation efficiency only if the average scratch separation d is comparable to the scratch width. Intuitively, this is understandable because then the rubbed grooves are completely overwritten by the SFM-made scratches.

We used scratching for the micromechanical fabrication of refractive index patterns in LC layers acting as waveguides. To fabricate a waveguide, we scratched a pattern (Fig. 4) on one plate of an LC cell. Region 1 was only rubbed in x direction, and region 2 was scratched in y direction. One obtains a parallel LC configuration in region 1 and a twisted configuration in region 2 (Fig. 2). Let us first concentrate on the region near the modified surface: In region 1, the nematic director (and thus, the molecules) aligns parallel to the rubbing direction. In region 2, the director aligns parallel to the SFM scratches in y direction. The refractive index of the LC is larger for light polarized parallel to the molecular axis than for light perpendicular to it. Light polarized in the y direction therefore sees a higher index of refraction in region 2 compared to region 1; thus, region 2 acts as an optical waveguide.

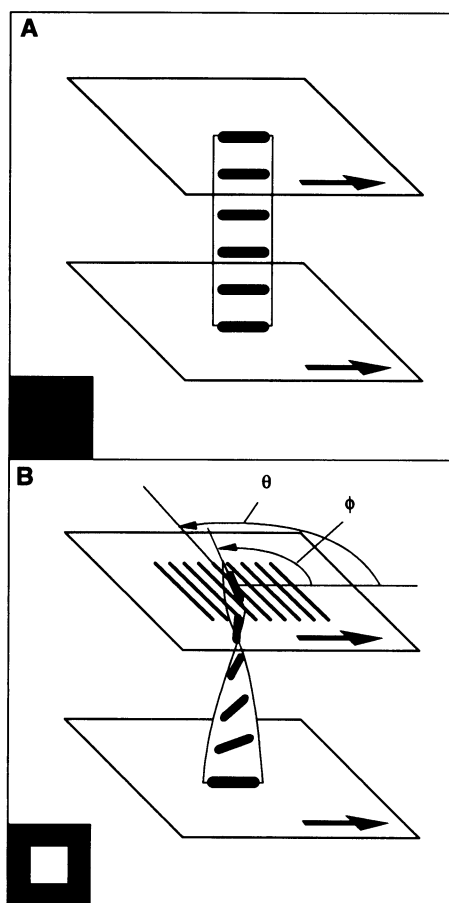


Fig. 2. Schematic comparison of LC alignment in an LC cell. The rubbing direction of each plate is indicated by an arrow. (A) Two rubbed plates without scratches. The LC molecules are aligned parallel to the rubbing directions of both plates. As a result, the polarization of transmitted light that is polarized parallel to the rubbing direction is not affected. (B) The upper plate after being scratched at an angle θ to the rubbing direction. The LC molecules near the scratched surface change their orientation in favor of the scratch direction, inducing a TN structure of the LC molecules in the bulk. As a consequence, the polarization of the light is rotated by an angle ϕ , which leads to a bright display. The expected displays are shown in the bottom left corners.

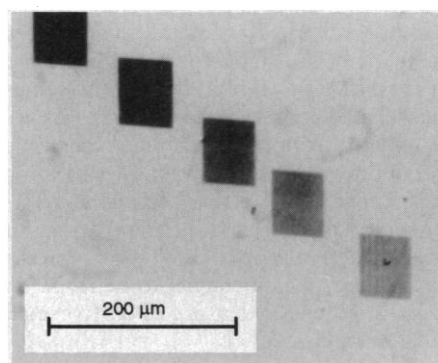


Fig. 3. Image of an LC cell obtained by means of a polarizing microscope. The dark rectangles are regions scratched by the SFM at a force of 10^{-7} N. The scratches are separated by $d = 135$ nm (not visible in the photograph). The scan velocity was doubled for each square from left to right, starting with $v = 0.4$ mm/s. The orientation of polarizer and analyzer were selected to achieve maximum extinction for the square with the highest orientation efficiency. The orientation efficiency clearly decreases with increasing scan speed.

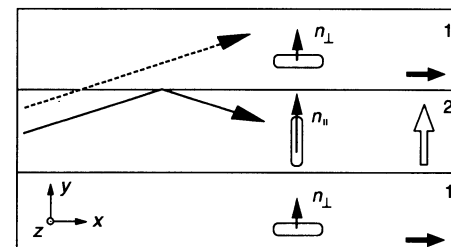


Fig. 4. An SFM-induced refractive index pattern that leads to an optical waveguide. Bold arrows in region 1 indicate the rubbing direction, and the open arrow in region 2 represents the scratching direction of the SFM. The index of refraction for a polarization perpendicular and parallel to the director are indicated by n_{\perp} and n_{\parallel} , respectively. Light polarized in the z direction passes undisturbed from region 2 to 1 (dashed line), whereas light polarized in the y direction is reflected at the interface between 2 and 1 (solid line).

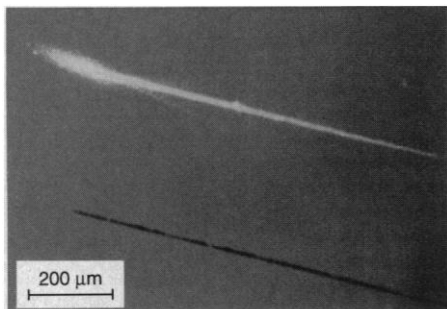


Fig. 5. An optical micrograph of the realization of two waveguides scratched according to Fig. 4. A laser beam is coupled into the upper one, leading to a bright streak of collimated light as a result of the waveguiding properties. The waveguides are 6 μm wide and 5 mm long.

What happens to the refractive index as one moves perpendicularly in z direction, away from the scratched surface? In region 2, the refractive index in the y direction decreases with increasing z because of the TN alignment of the LC molecules. Light cannot escape in the z direction because it is bent back, analogous to a graded-index waveguide.

We fabricated such structures (Fig. 4) with the home-built instrument by scratching a suitable pattern 6 μm wide and 5 mm long. To prevent the formation of reverse twist domains, we selected θ slightly smaller than 90° . The light-guiding property of this structure was deduced from the observation of a streak of light when a laser beam was suitably coupled into it (Fig. 5). The fabrication of this waveguide demonstrates that we can design bulk refractive index patterns by well-defined scratching patterns made with the SFM. Preliminary results on the possibility of fabricating coupling gratings, beam splitters, and other optical structures indicate that the smallest dimension of index patterns feasible is determined by elastic properties of the LC molecules as well as inhomogeneities of the polymer substrate but not by the size of the scratched areas.

We expect that this technique of writing an orientation pattern with a tip of an SFM will trigger the development of new devices because it offers a flexibility in shaping refractive index profiles that is unmatched by other techniques, such as photolithography-based pattern generation. The possibility provided by the SFM patterning technique to form arbitrarily complex two- or even three-dimensional refractive index patterns will certainly find further applications.

REFERENCES AND NOTES

1. K. Schmitt *et al.*, *Liq. Cryst.* **14**, 1735 (1993); K. Schmitt *et al.*, *J. Phys. III* **4**, 387 (1994).
2. For a review, see D. Rugar and P. Hansma, *Phys. Today* **43**, 23 (October 1990).
3. D. W. Berreman, *Phys. Rev. Lett.* **28**, 1683 (1972);

- J. M. Geary *et al.*, *J. Appl. Phys.* **62**, 4100 (1987); J. A. Castellano, *Mol. Cryst. Liq. Cryst.* **94**, 33 (1983); E. S. Lee, Y. Saito, T. Uchida, *Jpn. J. Appl. Phys.* **32**, L1822 (1993).
4. Th. Jung *et al.*, *Ultramicroscopy* **42**, 1446 (1992); E. Hamada and R. Kaneko, *ibid.*, p. 184; R. Kaneko and E. Hamada, *Wear* **162**, 370 (1993); X. Jin and W. N. Unertl, *Appl. Phys. Lett.* **61**, 657 (1992); O. M. Leung and M. C. Goh, *Science* **255**, 64 (1992).
5. H. Kado, K. Yokoyama, T. Tohda, *Rev. Sci. Instrum.* **63**, 3330 (1992).

6. Nanoscope III from Digital Instruments, Santa Barbara, CA.
7. The authors thank R. Lüthi, H. Haefke, L. Howald, and E. Meyer for helpful discussions. P.G. thanks the Treubel Fonds, Basel, for generous financial support. This research is supported by the Swiss National Science Foundation and the Kommission zur Förderung der wissenschaftlichen Forschung.

14 March 1994; accepted 31 May 1994

Measurement of Laser-Plasma Electron Density with a Soft X-ray Laser Deflectometer

D. Ress,* L. B. DaSilva, R. A. London, J. E. Trebes, S. Mrowka, R. J. Procassini, T. W. Barbee Jr., D. E. Lehr

A soft x-ray laser (wavelength $\lambda = 15.5$ nanometers) was used to create a moiré deflectogram of a high-density, laser-produced plasma. The use of deflectometry at this short wavelength permits measurement of the density spatial profile in a long-scalelength (3 millimeters), high-density plasma. A peak density of 3.2×10^{21} per cubic centimeter was recorded.

A detailed knowledge of the electron density spatial distribution in a laser-produced plasma is required in a wide range of scientific endeavors such as inertial confinement fusion (1), laser-plasma interaction physics (2), and high-temperature and high-density laboratory astrophysics (3). Density information is currently obtained with such diverse techniques as x-ray spectroscopy (4), absorption and scattering of incident laser light (5), and ultraviolet interferometry (6). All of these techniques are useful over only a limited range of densities and scale sizes, and they have additional limitations. Measurements based on x-ray spectroscopic techniques suffer from uncertainties in opacity and usually require sophisticated modeling of the atomic processes occurring in the plasma to infer a density. Measurements based on laser-light scattering require an understanding of one or more parametric instabilities produced by the laser creating the plasma under study. Ultraviolet interferometry is restricted to density length products less than $2 \times 10^{19} \text{ cm}^{-2}$, forcing high-density measurements to be made on plasmas with sizes that are often too small to be of interest.

To overcome some of these limitations, we have developed a technique based on moiré deflectometry (7) with a soft x-ray laser beam. We used this method to measure the electron density profile in a 3-mm-

diameter laser-produced plasma. The maximum density length product measured was $9.6 \times 10^{20} \text{ cm}^{-2}$, about 50 times higher than could be measured with conventional ultraviolet interferometry. The line-averaged peak density of $3.2 \times 10^{21} \text{ cm}^{-3}$ was limited by diffraction effects associated with the steepness of the density profile. Higher densities can be accessed by modifying the experimental arrangement.

When a high-intensity ($I > 10^{13} \text{ W/cm}^2$) laser irradiates a solid target, a plasma is created. The transverse extent of these plasmas is determined by the laser spot size and typically varies from hundreds to thousands of micrometers in diameter. The index of refraction for light propagating through this plasma is given by

$$N = \sqrt{1 - n_e/n_c} \quad (1)$$

where n_e is the electron density, $n_c = 1.1 \times 10^{27}/\lambda^2$ is the critical electron density per cubic centimeter, and λ is the wavelength of the light in nanometers. Because the laser beam can only propagate in the plasma where $n_e < n_c$, we can readily distinguish two regions in the direction normal to the material surface. The overdense region is where $n_e > n_c$, and the corona is where $n_e < n_c$. In our experiments, we used a green ($\lambda = 527 \text{ nm}$) laser drive beam with $n_c = 4 \times 10^{21} \text{ cm}^{-3}$. In the corona, at densities close to but less than critical, the spatial profile maintains a constant shape (steady-state profile) that slowly moves outward from the disk surface at a speed on the order of 10^6 cm/s (8). At lower densities, the spatial profile changes with time in a self-similar fashion. The profile here is a decay-exponential with a scalelength that

D. Ress, L. B. DaSilva, R. A. London, J. E. Trebes, S. Mrowka, R. J. Procassini, T. W. Barbee Jr., Lawrence Livermore National Laboratory, Livermore, CA 94551-5508, USA.
D. E. Lehr, Physics Department, Stanford University, Stanford, CA 94305, USA.

*To whom correspondence should be addressed.